LIQUID THERMAL DIFFUSION IN A BATCH ROTARY COLUMN

T.R. BOTT,[1]
J.de D.R.S. PINHEIRO,[2]

1. Chemical Engineering Department, The University of Birmingham, Birmingham, U.K.
2. Centro de Química Pura e Aplicada da Universidade do Minho, Braga, Portugal

ABSTRACT

Experimental observations of separation by thermal diffusion in rotary columns have been published, but no adequate theory to explain the column perfomance has been given. By consideration of the hydrodymanics within the annular space an approximate theory has been developed wich shows that for a geometrically perfect column the relevant parameters affecting separation can be simply related to the corresponding static column. The relaxation--time and separation are virtually independent of the speed of rotation and separation values are more favourable for the rotary column. The application of the theory to non-perfect pratical colums requires the consideration of the " equivalent annulus width " concept similar to the static case. Experimental tests conducted at different speeds of rotation in two geometrically different columns whose inner cylinder rotates and the outer is static, showed that the rotation at moderate speeds increased the equilibrium separation by about 7%, reducing, simultaneously the relaxation time by an average of 3%. These results are in good agreement with the theoretical predictions.

INTRODUCTION

Since Clusius and Dickell[(1)] introduced the thermogravitational thermal diffusion column, several modifications on the basic design have been proposed aiming at a better perfomance of the apparatus, i.e. larger degrees of separation or smaller separation times.

More recently, the interest of some investigators has been focused on the so-called."rotary column"- a concentric cylinder apparatus in which one or both cylinders may rotate about the common axis. Yet, in spite of some experimental and theoretical studies that have been reported in the literature[(2-5)] it has not been possible to appreciate adequately the separation potential of the rotary column or even to draw clear conclusions about the influence of the process variables on the overall efficiency. The reasons are to be found on the lack of agreement between the experimental results so far reported and the apparent inadequacy of the theoretical models that have been suggested.

In the present work an attempt is made to obtain some information which may help to clarify the situation. The two essential aspects under consideration are : -

1. Development of a phenomenological model similar to (and based on) the conventional thermogravitational theory by Furry, Jones and Onsager[(6)] (FJO)
2. Experimental investigation of the influence of the speed of rotation in the laminar regime below the critical Taylor Number.

The first objective requires, in the first place, a strategy to tackle the problem since the unique characteristics of the 3-dimensional transport in the rotary column virtually excludes the possibility of a simple analytical integration

of the resulting non-linear partial differential equation of continuity for mass transport.

It would appear that the suggestion of Romero[2] to reduce the problem to 2-dimensions through the introduction of some simplifying assumptions, so that a derivation-pattern analogous to that of the thermogravitational column could be followed is, in fact, a realistic compromise which, once accomplished, would enable the translation of conventional methods of design and optimization to the 3-dimensional rotary apparatus. The procedure requires, though, a somewhat detailed analysis of the existing physical situation, namely the hydrodynamics involved.

2. THE HYDRODYNAMICS

2.1 The velocity profiles and flow-path.

In a rotary thermal diffusion column the convective fluxes are of two types : -

1. Vertical natural convection originated by the thermal gradient across the width of the annulus.
2. Tangential forced convection caused by the rotation of one or both of the cylinders.

The profiles of the velocity components corresponding to the above convective fluxes may be obtained from the Navier-Stokes equations which, for the laminar flow of an incompressible Newtonian fluid at the steady-state are, in the coordinate system shown in fig 1 :

$$\frac{\delta}{\delta z}(\rho v) = 0 \qquad \ldots\ldots(1)$$

$$\frac{\delta P}{\delta x} = 0 \qquad \ldots\ldots(2)$$

$$\eta \frac{\delta^2 v_y}{\delta x^2} = 0 \qquad \ldots\ldots(3)$$

$$\eta \frac{\delta^2 v_z}{\delta x^2} = \frac{\delta P}{\delta z} + \rho g \qquad \ldots\ldots(4)$$

Assuming the wall velocites to be V_h and V_c, the boundary conditions are

$$v_y = V_h, \quad v_z = 0 \quad \text{at } x = -+\omega \qquad \ldots\ldots(5)$$

$$v_y = V_c, \quad v_z = 0 \quad \text{at } x = -\omega \qquad \ldots\ldots(6)$$

$$\int_{-\omega}^{+\omega} v_z \, dx = 0 \qquad \ldots\ldots(7)$$

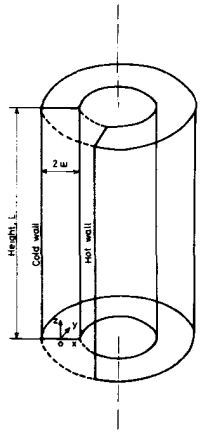

Fig. 1 - Concentric cylinder thermal diffusion column.

Equations (3) and (4) can be integrated separately and using the above boundary conditions the following well known solutions are obtained(*)

$$v_y = \frac{V_h - V_c}{2\omega} x + \frac{V_h + V_c}{2} \qquad \ldots\ldots(8)$$

$$v_z = \frac{\beta g (\Delta T)}{12 \eta \omega} * (\omega^2 - x^2) \qquad \ldots\ldots(9)$$

in which ω is the half distance between the walls, β is the temperature coefficient of density, η is the viscosity coefficient, g is the gravitational acceleration and (ΔT) is the temperature difference between the hot and cold walls.

The combination of these two components yields a resultant velocity, $v_R(x)$, which has a magnitude of

---

* FOOTNOTE

It is considered that $\frac{\delta T}{\delta x} = \frac{\Delta T}{2\omega}$ in accordance with the conclusions of TACHIBANA et al.[7]

$$v_R(x) = \sqrt{v_y^2 + v_z^2} \qquad \ldots\ldots(10)$$

and makes an angle $\psi(x)$ with the horizontal xy-plane defined by

$$\tan\psi(x) = \frac{v_z}{v_y} \qquad \ldots\ldots(11)$$

$$\sin\psi(x) = \frac{v_z}{\sqrt{v_y^2 + v_z^2}} \qquad \ldots\ldots(12)$$

Equations (8) to (12) are, in fact, the mathematical representation of a physical situation of which the following aspects must be emphasised:

1. The rotation deflects the particles streamlines from the vertical forcing them to follow a helical-path, the inclination of which, like the local velocity, is a function of the x-distance.

2. The vertical component, $v_z(x)$, is independent of the rotation and therefore the residence-time t_p - taken as the time required for a particle to travel from the top to bottom of the column or vice-versa- is not altered.

3. The column length being, indeed, the length of the particicle streamlines is not constant but rather a function of the x-distance. Hence, noting that t_p is constant and representing the length of the rotary streamlines by L* it is possible to write for a column of a vertical height of L:

$$\frac{L}{|v_z|} = t_p = \frac{L^*}{|v_R|} \qquad \ldots\ldots(13)$$

or, using equations (10) and (12) :

$$L^* = \frac{L}{|\sin\psi|} \qquad \ldots\ldots(14)$$

4. By substituting for the variables involved in equations (11), (8) and (9), specific values it may be readily seen that even for low speeds of rotation (of the order of, 5 RPM) the angle ψ is close to zero (*). As a consequence, the magnitude of the local velocity, v_R, and the local shear rate $\delta v_R/\delta x$ are practically identical to the corresponding local magnitudes of the tangential component:

$$|v_R| = |v_y|\sqrt{(\tan\psi)^2+1} = |v_y| \qquad \ldots\ldots(15)$$

$$\frac{\delta v_R}{\delta x} = \sin\psi\frac{\delta v_z}{\delta x} + \cos\psi\frac{\delta v_y}{\delta x} = \frac{\delta v_y}{\delta x} \qquad \ldots(16)$$

2.2 Types of rotary columns

A characteristic of the free-convection profile given by equation (9) is that, whatever the values of the variables involved may be, v_z is always an-odd-function of x, i.e.

$$v_z(+x) = -v_z(-x) \qquad \ldots\ldots(17)$$

which is equivalent to saying that the free convection streams for $x > 0$ and < 0 move countercurrently.

The same, however, is not true for the tangential component $v_y(x)$ which depends on the actual values of V_h and V_c . These may be combined in several different ways to which correspond different types of rotary flow patterns (simply designated by letters): -

Type A : Both walls rotate in the same direction with equal velocities

i.e, $V_h = V_c$

Type B : Both walls rotate in the same direction but with different velocities,

$V_h = V_c$, $V_h/V_c > 0$

---

*FOOTNOTE

For a column with one wall rotating with a speed N(r.p.m.) and assuming the followings CGS values for the variables : $\beta \sim 10^{-3}$, $g \sim 10^{3}$, $r \simeq 3$, $2\omega = 0.06$, $T = 20$ and making $\varepsilon = x/\omega$ the numerical value of tan ψ is approximately given by

$$|\tan\psi| \simeq \left|\frac{\varepsilon(1-\varepsilon)}{N}\right|$$

Type B_o: A subtype of the previous case in which one wall is static, $V_c = 0$ or $V_h = 0$

Type C : The walls rotate in opposite directions with the same absolute velocity , $V_h = - V_c$

Type C : The walls rotate in opposite directions with the same absolute velocity, $V_h = -V_c$

Type D : The walls rotate in opposite directions but with different velocities , $V_h = - V_c$, $V_h / V_c < 0$

Form equation (8) it may be easily seen that only type C corresponds to a profile that is an odd-function of x, i.e., only the tangential profile of type C is of true countercurrent nature relative to x=0. All the other cases, thus, have a combination of a tangential co-current profile with a vertical countercurrent profile. The net result, however, must be considered as a countercurrent--type process since it is clear that each atream contacts "fresh" fluid as it moves inside the annulus (see Fig.2).

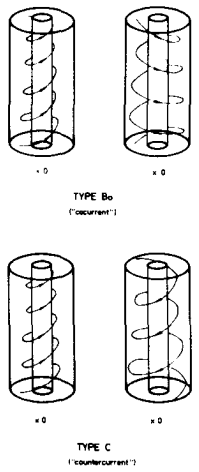

Fig.2 - Flow-paths in rotary columns

The fact that the overall flow inside a rotary column may be considered of the countercurrent type is of primary importance from the viewpoint of using the existing 2-dimensional derivation pattern which is based on that type of flow symmetry.

3. EARLIER WORK

3.1 Experimental reports

So far, it would seem that only columns of type B_o have been used experimentally. The first report was by Sullivan and co-workers[5] who , however, appeared to have worked at speeds above the critical Taylor Number and therefore out of the scope of the present work. A more detailed study at speeds below the critical Taylor Number was reported by Romero[2,8] who claimed that the rotation decreased the separation-time without increasing, though, the separation attainable. Romero also observed that the equilibrium separation decreased as the speed of rotation increased. A somewhat different conclusion was reached by Bott[3,9] who, using a column identical to Romero's but with a larger annulus width, noted that in the transient period of the separation (broadly, in the regious where the Ruppel--Coull[10] equation applies) the rotation increased the separation, the largest degree of separation being obtained for the higher speed of rotation studied.

Meanwhile, theoretical studies by Yeh and co-workers[4] suggested that a large increase in the degree of separation should occur where one of the cylinders rotates. (This work is discussed in the next section).

3.2 Theoretical studies

The first attempt to derive a phenomenological theory for the rotary column was by Romero[2]. This author rationalised the problem through an "elementary theory" in which the problem dimensions were reduced by neglecting the natural convection as compared to the forced convection and substituting the rotary column by a parallel plate one with the walls set in opposite motion. In the nomenclature of the present work, the substituition is equivalent to use type C instead of type B_o, keeping the rate of shear across the annulus unchanged.

Neglecting v_z in comparison with v_y is acceptable if the effect of v_z on the shape of the particles streamlines is taken into account. This Romero does in a clear discussion of the physical situation involved but somewhat surprisingly , the author uses for the column length the vertical height . As a consequence the theory predicts

degrees of separation far lower than those obtained experimentally.

Using the substitution of a type B_0 column by a type C one is acceptable from the viewpoint of Romero - the development of a " first approach " to the rotary column - although they are not strictly equivalent.

A more recent study has been presented by Yeh and Cheng[3] who developed a phenomenological model for continuous rotary columns(*) whose basic characteristics were :-

1. The introduction of the Brinkman Number , N_{Br}, - defined as $N_{Br} = \frac{\eta V^2}{k(\Delta T)}$ (where k is the thermal conductivity of the mixture) - to account for the distortions in the temperature profile (and consequently on the velocity profile) caused by the viscous heat generation.
2. The use of the "wired column" approach to derive the rotary column equation. (The "wired column" is a concentric tube column in which a wire of diameter equal to the annulus width is helically wrapped along the inner cylinder forcing therefore the particles to follow a helical-path inside the annulus).

As far as the Brinkman is concerned, its introduction appears to be unrealistic since it may be easily demonstrated, by substituting the variables involved by common (usual) numerical values, that N_{Br} is negligible for the vast majority of conditions encountered in practice.

As to the second aspect - the analogy between rotary and wired columns - it is indeed restricted to the shape and length of the particles streamlines. Wide differences do exist in values of the local velocity, residence-time or local shear rate, as may be seen by comparing the rotary equations (15) and (16) with the corresponding "wired equations" (where "w" stands for "wired")

$$(v_R)_w = v_z \sin \psi_w \qquad \ldots\ldots(17)$$

$$\left(\frac{\delta v_R}{\delta x}\right)_w = \sin \psi_w \frac{\delta v_z}{\delta x} \simeq 0 \qquad \ldots\ldots(18)$$

Moreover, the application of the Yeh and Cheng approach to the batch operation predicts that the value of the equilibrium degree of separation is cncreased by a factor equal to $(1/\sin \psi)$ which is quite large even for moderate speeds of rotation and, indeed, not vindicated by the experimental results so far available.

Before finalising this section it is interesting to note that the approach of Yeh and Cheng is, ultimately, an attempt to reduce the problem dimensions though by quite a different technique from Romero's and apparently unaware of the latter

4. THE TRANSPORT EQUATION

4.1 Simplifying approximations

To obtain the rotary transport equation through a pattern similar to the FJO derivation for the static column, it is necessary to introduce some approximations so that only two spacial coordinates are required to describe the transport involved and, simultaneously, to substitute the actual velocity profile by an approximate function with an odd-symmetry with respect to the x-distance.

The first approximation is to consider that the rotary column length, L*, defined by equation (14) has a constant value which implies that the angle ψ must also be considered as a constant:

$$\psi = \psi_a = \text{constant}$$

Physically, the aproximation introduced means that the particles streamlines have a constant inclination (independent from x) and, as a consequence, the resulting velocity profile exists in a xy-plane that makes an angle ψ_a with the horizontal xy-plane. It may also be concluded that this xy-plane together with equations (15) and (8) fully described the velocity profile that results from the approximation introduced.

---

* FOOTNOTE

The distinction betwenn batch and continuous phenomenological theories is immaterial from the viewpoint of establishing a body of rotary concepts or parameters since the continuous theories are, in fact, extensions of the corresponding batch ones.

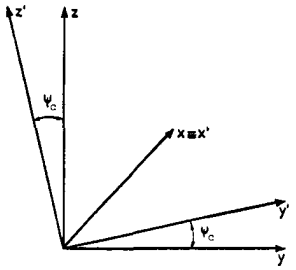

Fig.3 - Coordinate system x'y'z'

The actual value of ψ_a may be simply determined from the condition that the flowrates in the y and z directions are related by

$$\bar{v}_R \sin \psi_a \simeq \bar{v}_y \cdot \sin \psi_a = \bar{v}_z \qquad \ldots\ldots(20)$$

noting, now, that ψ_a is small and therefore sin $\psi_a \simeq \tan \psi_a$, the rotary length is

$$L^* = \frac{L}{|\sin \psi_a|} = \frac{L}{|\tan \psi_a|} = L.\frac{\bar{v}}{\bar{v}_y} \qquad \ldots\ldots(21)$$

It is worth emphasising that, at the present stage, the natural convection term, v_z, is neglected in evaluating the local velocity or shear stress i.e. similar to Romero's approach, but it is taken into account by defining a value $\psi_a \neq 0$.

The second basic approximation is related to the symmetry of the flow relative to the plane x=0 . First, it is considered that due to the countercurrent character of the "upwards" and "downwards" streams corresponding to the two column halves for x > 0 and x < 0 (briefly referred as x^+ and x^-). They are independent entities which only share a common boundary at x = 0. Secondly and in accordance with the approximation (19), the flow-rates in each half must be identical. Finally, it is also considered that within each half the sign of the shear stress is unimportant but rather its absolute value.

Under the above conditions it is possible to separate the rotary column into two halves having the velocity profiles shown schematically in fig 4 and 5 for columns of type A and B_o .
(see Fig 4)

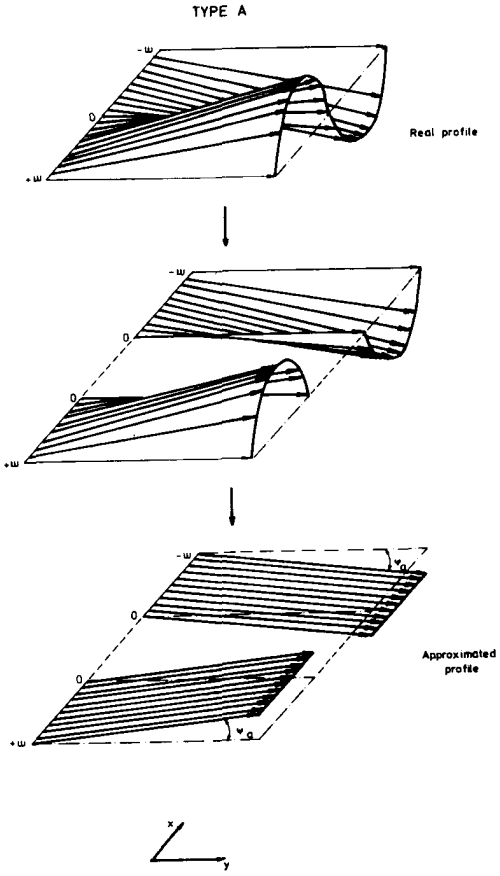

Fig.4 - Velocity profile in a rotary column of type A

Their mathematical representation is

$$v_y,(x^+) = \frac{V_h - V_c}{2\upsilon} x + \frac{V_h + 3V_c}{4} = R\omega(\varepsilon+A) \ldots(22)$$

$$v_y,(x^-) = \frac{V_h - V_c}{2\upsilon} x - \frac{V_h + 3V_c}{4} = R\omega(\varepsilon-A) \ldots.(23)$$

where $R = \frac{V_h - V_c}{2\omega}$

is the rate of shear across the annulus,

$$A = \frac{1}{2}\left(\frac{V_h + V_c}{R\omega} - 1\right) \qquad \ldots\ldots(25)$$

and

$$\varepsilon = \frac{x}{\upsilon} \qquad \ldots\ldots(26)$$

It is clear from equations (22) and (23) that the overall approximate profile is an odd--function of x.

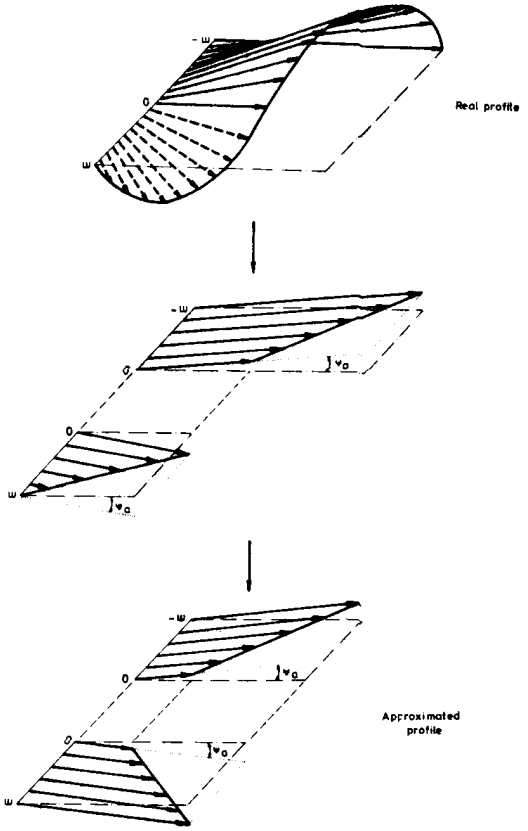

Fig.5 - Velocity profile in a rotary column of type B_o

4.2 The transport equation

In the xy'z' system of coordinates obtained from the xy system by rotating it around the x--axis by and angle ψ_a - see fig 3 - the velocity profile resulting from the approximations introduced has only one component : $v_{y'}(x)$. The mass fluxes existing in each half of the column have then the (usual) form

$$J_x = - \rho D \frac{\delta c}{\delta x} + \frac{\alpha \rho \; D(\Delta T)}{T_{av}(2\omega)} \; c \; (1-c) \qquad .....(27)$$

$$J_{y'} = \rho D \frac{\delta c}{\delta y'} + v_{y'} \; c\rho \qquad .....(28)$$

$$J_z = - \rho D \frac{\delta c}{\delta z'} \qquad .....(29)$$

in which c is the molar fraction of the specified component and T_{av} is the average absolute temperature inside the column, with the boundary conditions

$$J_x = 0 \quad \text{at} \quad x = \pm \omega \qquad .....(30)$$

$$c = c_o \quad \text{at} \quad t = o \qquad .....(31)$$

The equation of continuity is thus written as

$$\frac{\delta(c\rho)}{\delta t} = - \frac{\delta J_x}{\delta x} + \frac{\delta}{\delta y'} \; \rho D \frac{\delta c}{\delta y'} - v_{y'} \frac{\delta(c\rho)}{\delta y'} +$$

$$+ \frac{\delta}{\delta z'} \; \rho D \frac{\delta c}{\delta z'} \qquad .....(32)$$

In this form, equation (32) does not allow the FJO-approach to be followed due to the existence of the z' term which makes the equation 3-dimensional (in spacial terms). The problem may however be overcome by noting that, for small values of the angle ψ it is possible to assume that ($\delta c/\delta z$) ≃ ($\delta c/\delta z'$). Since the process may be "followed" either through the y' - direction or the vertical z - direction due to the helical shape of the streamlines, it is possible to write the approximate relationship

$$\frac{\delta c}{\delta z'} \simeq \frac{\delta c}{\delta z} \simeq \frac{L^*}{L} \; \frac{\delta c}{\delta y'} \qquad .....(33)$$

Using identical arguments for ($\delta\rho/\delta z'$) and noting that (L*/L) >>1, the equation of continuity becomes under these conditions

$$\frac{\delta(c\rho)}{\delta t} = - \frac{\delta J_x}{\delta x} + \frac{\delta}{\delta y'} \left[\rho D \left(\frac{L^*}{L} \right)^2 \frac{\delta c}{\delta y'} \right] -$$

$$- v_{y'} \frac{\delta(c\rho)}{\delta y'} \qquad .....(34)$$

This equation is a function of only two spacial dimensions (x and y') and is formally similar to the continuity equation obtained by FJO for the static column and with the same boundary conditions which means that hereafter it is possible to follow the classical derivation pattern.

Without entering into details which have been fully described in the literature[6,11,12] it suffices to say that the conventional derivation

arrives at an equation - the transport equation - - to describe the transport of the reference component along the column of the type

$$\tau = H\, c\,(1-c) - k\,\frac{\delta c}{\delta y} \qquad \ldots\ldots(35)$$

where τ is the mass flow-rate of the specified component and H and K, designated by "transport coefficients" have the following expressions

$$H = \frac{B\,\rho\,\alpha\,(\Delta T)}{T_{av}\,(2\omega)} \int_{-\omega}^{+\omega} G(x)\,dx \qquad \ldots\ldots(36)$$

$$K = K_c + K_d \qquad \ldots\ldots(37)$$

$$K_c = \frac{B\rho}{D} \int_{-\omega}^{+\omega} G(x)^2\,dx \qquad \ldots\ldots(38)$$

$$K_d = B\,\rho\,D(2\omega) \qquad \ldots\ldots(39)$$

where B is the column width in the y-direction and G(x) is an auxiliary function introduced in the derivation and such that

$$\frac{\delta\,(c\rho)}{\delta y'} \cdot G(x) = J_x \qquad \ldots\ldots(40)$$

and

$$\frac{\delta}{dx}\,G(x) + v_{y'} = 0 \qquad \ldots\ldots(41)$$

Also according to condition (30) and equation (40)

$$G(+\omega) = G(-\omega) = 0 \qquad \ldots\ldots(42)$$

In the present case the derivation is carried out independently for the two halves ($x \geq o$ and $x \leq o$) subjected to the condition:

$$J_x(x^+) = J_x(x^-) \text{ at } x=o \qquad \ldots\ldots(43)$$

or, in accordance with equation (40)

$$G(x^+) = G(x^-) \text{ at } x=o \qquad \ldots\ldots(44)$$

The overall transport of the specified component is thus the sum of the contributions of each half:

$$\tau = \int_0^{+\omega} J_{y'}(x^+)\,dx + \int_{-\omega}^{o} J_{y'}(x^-)\,dx =$$

$$= H^*\,c(1-c) - K^*\,\frac{\delta c}{\delta y'} \qquad \ldots\ldots(45)$$

The principal differences from the static theory of FJO concern the auxiliary function G(x) which, for the profiles described by equations (22) and (23) and in accordance with conditions (41) (42) and (44), has the form:

$$G(x^+) = \frac{-R\omega^2}{2}\left[\,\varepsilon^2 + 2A\varepsilon - (2A+1)\,\right] \ldots(46)$$

$$G(x^-) = \frac{-R\omega^2}{2}\left[\,\varepsilon^2 - 2A\varepsilon - (2A+1)\,\right] \ldots(47)$$

After performing the integrations indicated in equations (36) and (38) the following expressions are obtained for the transport coefficients of a rotary parameters: (the absence of asterisk identifies the static ones):

$$H^* = \frac{B^*\rho\,(\Delta T)}{T_{av}\,(2\omega)}\,\frac{R\,\omega^3}{3}\,(2+3A) \qquad \ldots\ldots(48)$$

$$K_c^* = \frac{B^*\rho}{D}\,\frac{R^2\omega^5}{30}\,(8 + 25A + 20A^2) \qquad \ldots(49)$$

$$K_d^* = B^*\,\rho\,(2\omega)\left(\frac{L^*}{L}\right)^2 D \qquad \ldots\ldots(50)$$

The physical meaning of the terms involved in the rotary transport equation is analogous to the static one:- The term $H^*c\,(1-c)$ representing the contribution of the thermal diffusion effect to the transport of the specified component and the terms $K_c^*\,\frac{\delta c}{\delta y}$, and $K_d^*\,\frac{\delta c}{\delta y'}$, accounting, respectively, for the remixing effects of the convective currents and ordinary molecular diffusion.

As a " corolarium ", any conceptual relation between these or other phenomenological parameters of equivalent physical significance will have the same form in both rotary and static columns. By analogy, then, with the static theory

it is possible to obtain steady and unsteadystate solutions for the transport equation using the methods described by Majumdar[13] and others[10,14]. The corresponding final equations are presented in the next section.

5. SEPARATION EQUATIONS

5.1 Theoretical equations

By analogy with the static theory the following rotary parameters may be defined :

- Dimensionless length $\lambda^* = \frac{H^* L^*}{K^*}$ .....(51)

-Equilibrium separation $\Delta^*_\infty = \frac{(e^{c_o\lambda^*}-1)\ (e^{\lambda^*}-e^{c_o\lambda^*})}{e^{c_o\lambda^*}\ (e^{\lambda^*}-1)}$ .....(52)

-Relaxation-time $t^*_r = \frac{\mu^* K^*}{H^{*2}} \quad \frac{1}{\frac{1}{4} + \left(\frac{\pi}{\lambda^*}\right)^2}$ .....(53)

-Moles/unit of length $\mu^* = B^* \rho\ (2\omega)$ .....(54)

-Dimensionless time $\theta^* = \frac{H^{*2}}{\mu^* K^*} t$ .....(55)

For large values of time such that $t > 0.3 t^*_r$ the solution of the transport equation by Hoffman and Emery[14] yields the following equation for the dependence of the degree of separation, Δ^*, on the values of Δ^*_∞ , t^*_r and t:

$$\Delta^* = \Delta^*_\infty \left(1 - \frac{8}{\pi^2}\ e^{-t/t^*_r} \right) \qquad .....(56)$$

For short experimental times such the $\theta^* < 0.05 \left| \lambda^* \right|^{1.82}$, the dependence of the degree of separation, Δ^* , on the variables involved may be obtained from the solution presented by Ruppel and Coull[10] for the static case. The equation is: (The subscript RC stands for "Ruppel and Coull"):

$$\Delta^*_{RC} = 4\ c_o(1-c_o) \sqrt{\frac{\theta^*}{\pi}} = s^* \sqrt{t} \qquad ...(57)$$

with

$$s^* = \delta\ \Delta^*_{RC} \ /\ \delta\sqrt{t} \qquad .....(58)$$

i.e.s^* is the critical slope of the curve relating Δ^*_{RC} and $\sqrt{t}$.

For columns of type B_o the value of the parameter A defined by equation (25) is 1/2 and the value of L* defined by equation (21) may be obtained using equations (8) and (9):

$$L^* = 96\ \frac{\eta\ V\ L}{\beta g\ (\Delta T)(2\omega)^2} \qquad .....(59)$$

The phenomenological parameters involved in the separation equations (56) and (57) may now be determined from equations (48) (49) and (59):

$$\lambda^* = 527.1\ \frac{\alpha\ D\ \eta\ L}{\beta g\ T_{av}(2\omega)^4} = 1.046\ \lambda \qquad ...(60)$$

$$t_r = 1.25 \left[\frac{T_{av}\ (2\omega)}{\alpha\ (\Delta T)\sqrt{D}} \right]^2 \quad \frac{1}{0.25 + \pi^2/\lambda^2} =$$

$$= 0.875 \left[\frac{0.25 + \pi^2/\lambda^2}{0.25 + \pi^2/\lambda^{*2}} \right] \cdot t_r \qquad .....(61)$$

$$s^* = 2.019\ \frac{c_o\ (1-c_o)\ \alpha\ (\Delta T)\sqrt{D}}{T_{av}\ .\ (2\omega)} = 1.068\ s \qquad (62)$$

Equations (60) and (62) respectively show that s^* , λ^* (and, hence Δ^*_∞) are larger than the corresponding static parameters. In contrast the rotary relaxation-time t^*_r is smaller than the static one as shown by equation (61). On the whole, therefore, it may be conclued that the theory predicts the perfomance of rotary columns of type B_o is better than the perfomance of a static column under the same experimental conditions although the improvement is moderate. If the procedure described for columns of type B_o ($A = \frac{1}{2}$) was carried out for the other types mentioned , the results would be similar in regard to the relaxation-time and the short-time separation,but would show significant differences in the ratio

λ^*/λ. A semi-quantitative comparison is shown in Table 1 where it may be appreciated that the lar - gest equilibrium separation attainable is for the type A column (both walls rotating in the same direction with equal velocities).

TABLE 1

Comparison between the theoretical performances of rotary and static columns

Type of column	$\frac{\lambda^*}{\lambda}$	$\frac{\Delta_{\infty}^*}{\Delta_{\infty}}$	$\frac{t_r^*}{t_r}$	$\frac{s^*}{s}$	$\frac{\Delta_{RC}^*}{\Delta_{RC}^*}$	Rotary performance relative to the static
A	1.143	>1	<1	1.034	>1	Better
B(Am1)	1.078	>1	1<	1.059	>1	Better
B_o	1.046	>1	1<	1.068	>1	Better
C	0.952	1<	1<	1.090	>1	Comparable

Another interesting aspect worth mentioning and somewhat surprising is the fact the phenomenological parameters are independent of the speed of rotation apart from the limitations imposed by the critical Taylor Number ("upper limit") and by the assumption that the angle ψ_a is small (" lower limit ").

In connection with the " lower limit " it is also of importance to note that the error involved in the simplifying approximations introduced decreases as the speed of rotation increases. Hence, the " lower limit " is defined by imposing a maximum value for the error. This means, on the other hand, that the separation equations derived are the asymptotic solutions which apply at speeds below $N = \infty$ with a certain degree of error which, in turn, is negligible at apeeds above the " lower limit ".

5.2 Equivalent annulus width of a rotary column

The assumption of a constant annulus width implicit in the FJO-approach is seldom acceptable when considering real columns due to the high $L/(2\omega)$ rations which because of constuctional difficulties, implies the existance of small eccentricities along the column height. This problem has been discussed by several authors [14,16] and ultimately has led to the introtuction by Bott and Romero[16] of the "equivalent annulus width" concept - the annulus width of a geometrically perfect column which yields the same separation as the actual imperfect one under the same experimental conditions. This concept was further developed by Romero and Pinheiro[17] who proposed a method for the evaluation of the " equivalent annulus width " which is discussed below.

The introduction of the concept for the static column was essentially based on hydrodynamical considerations which, however, may not be strictly applied to the rotary case mainly because the spacial location of the "funnels" originated by the eccentricities are continuously displaced by the rotation, It may, though, be admitted that a certain degree of instability is transmitted to the flow by the eccentricities and therefore one must accept that the overall perfomance of the column is affected. Whether or not an " equivalent annulus width " for the rotary column may be defined by analogy with the static column is a question whose answer requires the application of the Romero and Pinheiro[17] method to the experimental data abtained.

The method derived for the static column allows the independent evaluation of the equivalent annulus width and thermal diffusion factor and is simply based on the fact that the static parameters λ and s may be written as

$$s = \frac{\alpha}{2\omega} \cdot m \qquad \ldots\ldots(63)$$

$$\lambda = \frac{\alpha}{(2\omega)^4} \cdot n \qquad \ldots\ldots(64)$$

where

$$m = 1.89 \frac{c_o(1-c_o)\ (\Delta T)\sqrt{D}}{T_{av}} \qquad \ldots\ldots(65)$$

and

$$n = 504 \frac{D\ \eta\ L}{\beta g\ T_{av}} \qquad \ldots\ldots(66)$$

The coefficients m and n may be evaluated separately with accuracy independent from α and (2ω), and the values of s and λ may be determined experimentally. Under these conditions,

equations (63) and (64) form a system of 2 equations with 2 unknowns whose solution is

$$2\,\omega = \left(\frac{n\,s}{m\,\lambda}\right)^{\frac{1}{3}} \qquad \ldots\ldots(67)$$

$$\alpha = 2\omega \cdot \frac{s}{m} = \frac{s}{m} \cdot \left(\frac{ns}{m\lambda}\right)^{\frac{1}{3}} \qquad \ldots\ldots(68)$$

In the rotary case the basic differences are in the numerical factors of equations (65) and (66) which become, in accordance with equations (60) and (62):

$$m^* = 2.019\,\frac{c_o\,(1-c_o)\,(\Delta T)\sqrt{D}}{T_{av}} \qquad \ldots\ldots(69)$$

$$n^* = 527.1\,\frac{D\,\eta\,L}{\beta g\,T_{av}} \qquad \ldots\ldots(70)$$

and

$$(2\,\omega^*) = \left(\frac{n^*\,s^*}{m^*\,\lambda^*}\right)^{\frac{1}{3}} \qquad \ldots\ldots(71)$$

$$\alpha = \frac{s^*}{m^*}\left(\frac{n^*\,s^*}{m^*\,\lambda^*}\right)^{\frac{1}{3}} \qquad \ldots\ldots(72)$$

It is seen that to examine the adequacy of the " rotary equivalent annulus width " is also to examine the separation equations in which its evaluation is based. This adequacy may however be tested in two complementary ways :

- By comparing the value(s) of α obtained from equations (32) with others cited in the literature.

- By comparing the experimental separation curve with the two theoretical curves obtained using:

a) The equivalent annulus width given by equation (71)

b) The mechanically measured annulus width, $(r_2 - r_1)$.

6. EXPERIMENTAL WORK

6.1 Experimental apparatus and conditions

The experimental apparatus used in this work has already been described elsewhere [3,9] so that only the principle characteristics are described. It is comprised of two concentric cylinders made of brass, the height being 102 cm, the mechanically measured[3,9] annulus width 0.0571 cm and the annular volume 80cm^3. The inner cylinder may rotate at speeds up to 300 RPM while the outer cylinder is static. The heating and cooling of the walls is made through a thermostatic water circuit which flows inside the inner cylinder (hot wall) and through a water-jacket surrounding the outer cylinder (cold wall). The wall temperatures are measured through a group of 8 thermocouples placed in each wall at four different heights. The column is also provided with eleven sampling ports equally spaced along the height.

The test mixture used was n-heptane-benzene with an initial composition of $c_o = 0.560$ (molar fraction of benzene), each component being of high purity[18]. The analysis of the mixture composition was by refraetometry with an accuracy greater than 0.001 of the molar fraction.

The temperature difference between the walls was 18.5 ± 0.25°C and the average temperature 293 ± 2°K. The vertical variation of the temperature was in no case larger than 0.5°C.

The rate of sampling was 1 sample/run in accordance with the recommendations of Vichare and Powers[19], i.e. after a sample is withdrawn the column is emptied, washed with fresh mixture, emptied again and finally filled up with fresh mixture for a new run.

In the runs referred to as 1B the column was operated at full height (102 cm) and in the runs 2B with a height of 90 cm by leaving the upper section empty. This was intended as a means of assessing the influence of a suspected imperfect zone located near the top of the column (between L = 91 cm and L = 102 cm) on column efficiency.

Before assembling the column (which has self-aligning devices) the inner and outer cylinder diameters were carefully measured[8,9] at 9 different points equally spaced along the height.

The mechanically measured (or theoretical) annulus width is obtained by subtracting the cylinder radii at corresponding heights. The average values for the annulus width are listed in Table 2 for runs 1B and 2B and it is seen that it may be considered that two geommetrically different columns were used as shown in Table 2. The Table also shows the speeds of rotation at which the columns were operated.

TABLE 2

Column dimensions and operational velocities

	Height, L (cm)	$(r_2-r_1)_{av}$ (cm)	Speed of rotation, N (rpm)
COLUMN 1 (runs 1B)	102	0.0571	0, 1, 3, 6, 12, 28, 48, 88,
COLUMN 2 (runs 2B)	91	0.0565	0,1,3,10,20,44

6.2 Results and discussion

For each column and speed of rotation, the degree of separation, Δ , was determined for , at least, 13 different experimental times ranging from very short times of about 0.25 hrs up to times near equilibrium of the order of 30 hrs. or more. This set of (t_i, Δ_i) pairs constituted the input of computer programmes specially devised, whose output inclued the best valus - as determined by least squares methods - of the parameters λ^*, Δ^*_∞ , t^*_r and s^* (or λ, Δ_∞, t_r and s). The values of Δ^*_∞ and t^*_r are determined so that the (theoretical) curve of Δ^* vs. t obtained by substituting those values of Δ^*_∞ and t^*_r into equation (57), yields the minimum deviation between the experimental points (Δ^*_i , t_i) and the corresponding points in the theoretical curve (Δ^* , t). In this work , it was found that in no case was the deviation (*) greater than 5% which means that (with an error less than 5%) the experimental results are well described by the two values of Δ^*_∞ (or λ^*) and t^*_r given by the computer and presented in Tables 3 and 4 .

TABLE 3 Experimental and calculated parameters - column 1

N (RPM)	Δ^*_∞	λ^*	t^*_r (hr)	$s^*.10^2$ (min^{-1})	$2\omega .10^2$ (cm)	α	$\frac{\lambda^*}{\lambda}$
0	0.462	2.03	3.82	2.35	6.14	1.36	-
1	0.464	2.04	3.78	2.40	6.13	1.31	1.004
3	0.477	2.11	3.43	2.44	6.10	1.32	1.032
6	0.490	2.18	3.29	2.47	6.06	1.33	1.061
12	0.495	2.20	3.58	2.29	5.90	1.29	1.071
28	0.500	2.23	3.87	2.46	6.00	1.31	1.080
48	0.471	2.08	3.54	2.43	6.12	1.32	1.019
88	0.410	1.77	2.14	2.43	6.23	1.34	0.888

$m.10^3 = 1.056$ $m^*.10^3 = 1.128$ $n.10^5 = 2.11$ $n^*.10^5 = 2.21$

The values of λ^* and s^*, together with the values of m^*, n^*, m and n determined, respectively, from equations (69), (70), (65) and (66) using the appropriate values of the variables involved (c_o=0.560, ΔT=18.5°C, T_{av}=293.5°K, $\beta.10^3$=0.88 $g.cm^{-3}.{}^oC^{-1}$, $\eta.10^2$=0.461 $g.cm^{-1}.s^{-1}$, $D.10^4$=0.216 $cm^2.s^{-1}$, ρ=0.767 $g.cm^{-3}$, g=980 $cm.s^{-2}$) allow the evaluation of the "equivalent annulus width" and thermal diffusion factor using the method of Romero and Pinheiro described earlier. The results thus obtained are summarized in Tables 3 and 4 and suggest the following observations:-

1. Although in theory for a given speed of rotation column 1 equilibrium separation should be nearly 6% higher than that of column 2, it is seen that, in practice, it is of the order of 10% lower than the equilibrium separation obtained in column 2. This discrepancy must be attributed to the geometric irregularities existing near the top of column 1 which promote extra-remixing effects that affect the whole apparatus efficiency. Not surprisingly, therefore, the ratio between the equivalent annulus width, and mechanically measured gap, $2\omega/(r_2 - r_1)$, (which may be considered as a measure of the degree of imperfection of the column)-

* FOOTNOTE

The percentage deviation between the experimental ponts (Δ^*_i , t)and the theoretical value of separation, Δ^*, for the same value of the time, t_i is given by $\frac{\sqrt{(\Delta^* - \Delta^*_i)^2}}{\Delta^*_i}$

is considerably higher for column 1 for the same value of N as may be seen from the tables.

2. The values of the thermal diffusion factor, α, determined from the data of either column 1 or 2 show a very good agreement between themselves and with other values reported in the literature and determined in thermogravitational columns[17].

TABLE 4 - Experimental and calculated parameters - column 2

N (rpm)	Δ^*_∞	λ^*	t^*_r (hr)	$s^*.10^2$ ($min^{-\frac{1}{2}}$)	$2\omega.10^2$ (cm)	α	$\frac{\lambda^*}{\lambda}$
0	0.516	2.32	4.22	2.48	5.76	1.35	-
1	0.516	2.32	4.11	2.56	5.79	1.31	1.000
3	0.523	2.36	4.19	2.61	5.79	1.34	1.017
10	0.564	2.60	4.29	2.63	5.62	1.31	1.121
20	0.558	2.56	4.25	2.65	5.66	1.33	1.103
44	0.541	2.46	4.27	2.63	5.73	1.34	1.060

$m.10^3 = 1.056$ $m^*.10^3 = 1.128$ $n.10^5 = 1.89$ $n^*.10^5 = 1.98$

3. The equivalent annulus width, in both columns, appears to decrease first as the s speed increases, to reach a minimum and then to increase with increasing speeds of rotation. This suggests that the role of the geometric irregularities in a rotary column tend to become more important for higher speeds due probably to some local fluid instability arising at large values of the rotation.

Conversely, $\lambda^* \propto (2\omega)^{-4}$ reaches a relative maximum and then decreases monotonically as the speed of rotation increases as shown in Fig 6 through the experimental curves for column 1 (curve E_1) and column 2 (curve E_2).

By comparing the experimental λ^* vs. N curves (E_1 and E_2) with the theoretical curves predicted by the theory for perfect columns 1 and 2, (curves T_1 and T_2 , respectively, in fig 6) it is seen that for column 2 the twoo curves (E_2 and T_2) are not far apart in contrast to what happens to column 1 (E_1 and T_1). Furthermore the shape of the experimental curves suggest that may considered as distorted theoretical curves.

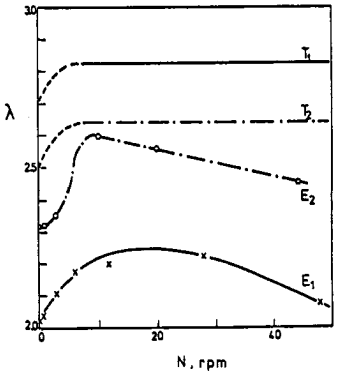

Fig. 6 - Comparison between experimental and theoretical values of parameter λ^*

T_1 - Theoretical curve for a perfect column 1

E_1 - Experimental curve for column 1

T_2 - Theoretical curve for a perfect column2

E_2 - Experimental curve for column 2

4. The existance of geometric imperfections with the need to consider "equivalent annulus widths" clearly alters the theoretical ratio of $\lambda^*/\lambda \simeq 1.05$ as shown by the last column in Tables 3 and 4. It is interesting to note, though, that, not only is that ratio larger than unity in all cases except for N=88 RPM in column 1, but also that the average value of that ratio ($\lambda^*/\lambda = 1.04$ for column 1 and $\lambda^*/\lambda = 1.06$ for column 2) are quite close to the theoretical value of 1.05.

5. The comparatively low separation obtained in column 1 for N = 88 RPM assumes a larger significance if it is noted that the "upper limit" of velocity, N^L, defined through the critical Taylor Number[20,21] is not far apart from the speed of 88 RPM:

$$N^L = \frac{(N_{Ta})_c}{\pi^2/900} \left[\frac{(r_2+r_1)\,\eta^2}{4\, r_1^2\, (2\omega)^3 \rho^2} \right]^{\frac{1}{2}} = 95 \text{ RPM} \qquad \ldots\ldots(73)$$

It is logical, therefore, that some degree of instability with a possible change of

flow regime may have occurred in the (imperfect) column 1 at that high speed.

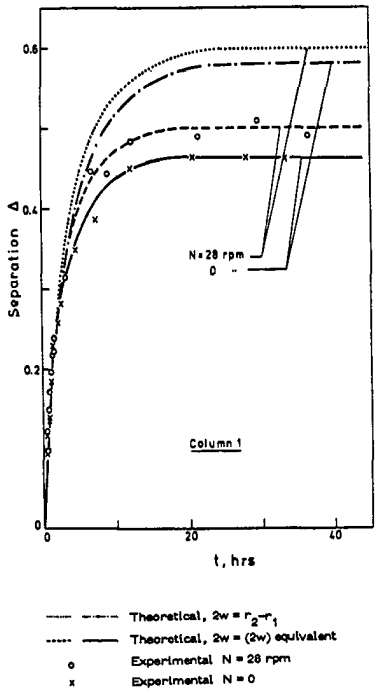

Fig. 7 - Typical comparisons between the theoretical curves (for $2\omega = r_2 - r_1$ and $2\omega = (2\omega_{equiv.})$ and the experimental points in column 1

The above comments generally suggest that the experimental results obtained show a trend that is in agreement with the theory derived earlier. The most meaningful test is , though, the comparison between the separation vs. time curve predicted by equation (56) and the experimental points. Typical examples of these comparisons are shown in figs. 7 and 8 in which two theoretical curves for each speed are represented: one using the " equivalent annulus width " and the other calculated for $2\omega = (r_2 - r_1)$. The comparisons for other speeds show similar trends which may be summarised as :-

1. The use of the "equivalent annulus width" in equation (56) produces a curve that has a much better agreement with the experimental points than the curve obtained from equation (56) using $2\omega = r_2 - r_1$. This is particularly true for column 1 and for the static operation of column 2.

2. In column 2 the two theoretical curves for N=0 are distinctly apart whereas for N=10 RPM the curves are close together sugesting that at this speed of rotation the irregularities are not so important as they become for N=0 or for higher speeds of rotation.

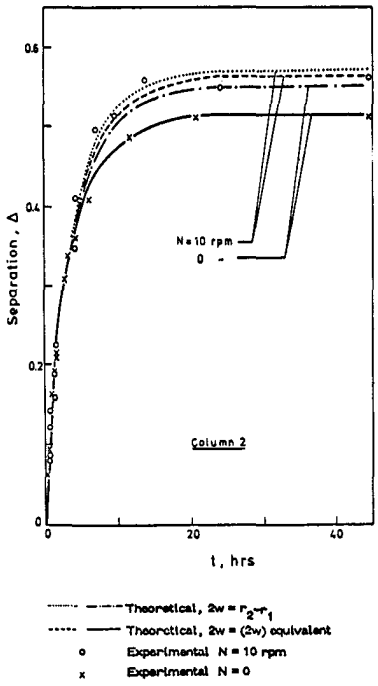

Fig. 8 - Typical comparisons between the theoretical curves (for $2\omega = r_2 - r_1$ and $2\omega = (2\omega_{equiv.})$ and the experimental points in column 2.

7. CONCLUSIONS

It is thought that the main conclusinos to be drawn from the present work may be summarised as follows:

1. The approximate phenomenological theory of the rotary thermal diffusion column derived using some simplifying approximations to reduce the problem dimensions and with an approach similar to that of FJO appears to describe satisfactorily the behaviour of a geometrically perfect column.

2. For real rotary columns (geometrically imperfect) it is necessary to consider, by analogy with the static column, an "equivalent annulus width" whose value may be determined by a method similar to the static case. When this rotary " equivalent annulus width " is used a good agreement is observed between theory and experiment (even for non-perfect columns).

3. The column efficiency improved when rotated at speeds up to about 50 RPM. The average increase in the equilibrium separation relative to the static operation was 6% and 7% for the two columns used. These figures agree fairly with the theoretical prediction of a 5% improvement.

AKNOWLEDGEMENT

The authors acknowledge, with sincere thanks, the provision of laboratory facilities by Professor J.T. Davies and the University of Birmingham in support of the research reported.

One of the authors (J.D.R.S. Pinheiro) wishes to express his gratitude to the Calouste Gulbenkian Foundation, Lisbon, Portugal for the provision of a scholarship which made this work possible.

NOTATION

A	parameter defined by eqn(25)
B, B^*	column width in the y and z directions, respectively
C	molar fraction of the reference component (benzene)
C_o	initial composition
D	ordinary diffusion coefficient
g	gravitational acceleration
G, G^+, G^-	auxiliary functions defined respectively by eqns (40), (46) and (47)
H, H^*	transport coefficients defined, respectively, by eqns(36) and (48)
J_k	mass flux of the reference component
K_c, K_c^*, K_d, K_d^*	thermal conductivity transport coefficients given by, respectively, eqns (38),(49),(39), and (50)
L	column height
L^*	lenght of the rotary column, defined by eqn (21)
m, m^*	coefficients defined by, respectively, eqns (64) and (68)
n, n^*	coefficients defined by, respectively, eqns (65) and (69)
N	speed of rotation of the inner cylinder in r.p.m.
N_{Br}	Brinkman Number, $N_{Br}=\eta V^2/k(\Delta T)$
N_{Ta}	Taylor Number, $N_{Ta}=4\pi^2 r_1^2 \rho^2 (2\omega)^3 N^2/900(r_1+r_2)\eta^2$
$(N_{Ta})c$	critical Taylor Number , $(N_{Ta})_c \simeq (3 \pm 0.3).10^3$
p	local pressure
r_1, r_2	cylinder radii
R	shear rate across the annulus, defined by eqn.(24)

s, s^*	initial slope of the separation vs. square root of the time curve given by eqn (61)
t	time
t_p	residence-time, defined by eqn (13)
t_r, t_r^*	relaxation-times defined in equation (60)
T	absolute temperature
v_i	velocity component (in the i-direction)
V_R	resultant velocity defined by eqn (10)
V_h, V_c	tangential velocities of the hot and cold walls
x, x'	horizontal coordinate normal to the walls surfaces
y	horizontal coordinate parallel to the walls surfaces
y'	coordinate direction defined in fig 3
z	vertical coordinate
z'	coordinate direction defined in fig 3

Greek symbols

α	thermal diffusion factor
β	temperature coefficient of density $= -(\partial\delta/\partial T)_p$
Δ, Δ^*	difference in composition between the top and bottom of the column
ΔT	temperature difference between the walls
ε	dimensionless horizontal distance defined by eqn (26)
η	viscosity of the mixture
θ	dimensionless time, defined by equation (55).
λ, λ^*	dimensionless length, defined , by eqns (51) and (59)
μ^*	no. of moles per unit length of the column
π	3.141592...
ρ	mass density of the mixture
τ	total transport of specified component in the direction of convection, eqn (35)
ψ	deflection angle of the particles streamlines from the horizontal plane
ψ_a	deflection angle defined by eqn. (20)
ω	one-half the distance between hot and cold walls

Subscripts

av	average
RC	"Ruppel and Coull"
x,x',y,y'	coordinate direction
w	wired column
∞	steady-state

Superscripts

*	rotary column
-	average (velocity)

REFERENCES

1. CLUSIUS,K.and DICKELL,G. Naturwissenschaften 1938,26,546
2. ROMERO, J.J.B Dechema-Monogr. 1971,65,337
3. BOTT, T.R. Chemeca 70,p.35, Butterworths, Australia 1970
4. YEH, H.M. and CHENG, S.M. Chem. Eng. Sci., 1973, 28,1803
5. SULLIVAN,L.J.,RUPPEL, T.C. and WILLINGHAM, C.B. Ind. Eng.Chem. 1955,47,208
6. FURRY, W.H.,JONES, R.C.and ONSAGER, L.Phys. Rev.1939, 55, 1083

7. TACHIBANA, F.,FUKUI, S. and MITSUMURA , H. Bull J.Soc. Mech.Engrs 1960,3,119

8. ROMERO, J.J.B. Ph.D. Thesis, Univ of Birmingham 1967

9. BOTT, T.R. Ph.D. Thesis, Univ of Birmingham, 1968

10. RUPPEL, T.C. and COULL, J. Ind. & Eng. Chem., Fundamentals 1964, 3 ,368

11. ROMERO, J.J.B Rev. Fis. Quim. Eng. ULM,1970, 2 A,1

12. POWERS, J.E. "Thermal Diffusion" in "New Chemical Engineering Separation Techniques", ed. Schoen Interscience Pub., 1962

13. MAJUMDAR, S.D. Phys. Rev., 1951,81,844

14. HOFFMAN, D. and EMERY, A.H. A.I.CH.E. Journal, 1963,9,653

15. KORCHINSKY, W.and EMERY, A.H. A.E.CH.E. Journal, 1967, 13, 224

16. BOTT, T.R. and ROMERO, J.J.B Trans. Instn. Chem Engrs 1969, 47,T166

17. ROMERO, J.J.B. and PINHEIRO, J.D.R.S. Chem.Eng. Sci., 1975, 30, 1459

18. PINHEIRO, J.D.R.S., PINHEIRO, H.M.P.S., ROMERO J.J.B. Rev. Fis. Quim. Eng : ULM,1973,5 A, 1

19. VICHARE, G.and POWERS, J.E. A.I.CH.E. Journal, 1961, 7 , 650

20. CHANDRASEKHAR, S.Mathematics, 1954, 1, 5

21. PINHEIRO, J.D.R.S. M.Sc. Thesis, Univ. of Birmingham, 1974

CHEMPOR '78

INTERNATIONAL CHEMICAL ENGINEERING CONFERENCE

University of Minho

Braga, Portugal

September 10–16 1978

CHEMPOR '78

REUNIÃO INTERNACIONAL DE ENGENHARIA QUÍMICA

Universidade do Minho

Braga, Portugal

Setembro 10–16 1978